Comprehensive and Practical Way to Look at Far-End Crosstalk for Transmission Lines With Lossy Conductor and Dielectric

Shaohui Yong , Student Member, IEEE, Victor Khilkevich, Member, IEEE, Xiao-Ding Cai , Member, IEEE, Chunchun Sui , Member, IEEE, Bidyut Sen, and Jun Fan , Fellow, IEEE

Abstract—Far-end crosstalk (FEXT) noise is one of the major issues that limits signal integrity performance for high-speed digital products. It is important to estimate the crosstalk noise accurately to avoid noise margin failure or overdesigned transmission lines. Traditionally, analytical formulas for crosstalk noise are based on lossless and perfect impedance match assumptions, which provide limited guidance for a practical high-speed transmission line design. A phenomenon is observed that a lossy conductor increases the FEXT on coupled striplines. To provide a reasonable explanation, analytical and numerical investigations were performed using a modal analysis based approach. A new FEXT component due to the lossy conductor is proposed. Such FEXT component is important to a high-speed stripline design because it is a major contributor when all terminals are matched. To estimate the impact of loss on FEXT, a practical and fast estimation approach is proposed.

Index Terms—Far-end crosstalk (FEXT), lossy conductor, proximity effect, serializer/deserializer (SerDes), transmission line theory.

I. INTRODUCTION

S THE data rate and density of digital high-speed systems are getting higher, the signal integrity (SI) performances of transmission lines are bottlenecked by the following three major issues: loss, impedance mismatch, and crosstalk noise. Nowadays, serializer/deserializer (SerDes) channels have already achieved speeds of 30+ Gbps with transmitted pulse rise time reduced to only several picoseconds. Issues brought by far-end crosstalk (FEXT) are not only more severe due to a shorter pulse rise time but also more complicated because of the crosstalk noise traveling in the transmission line with frequency-dependent attenuation. If FEXT is not well analyzed and predicted, SI engineers could either fail to meet the noise margin specifications resulting in a costly redesign or have

Manuscript received December 4, 2018; revised January 30, 2019; accepted February 21, 2019. Date of publication March 18, 2019; date of current version April 14, 2020. This work was supported in part by the National Science Foundation under Grant IIP-1440110. (Corresponding author: Jun Fan.)

S. Yong, V. Khilkevich, and J. Fan are with the EMC Laboratory, Missouri University of Science and Technology, Rolla, MO 65401 USA (e-mail: sy2m5@mst.edu; khilkevichv@mst.edu; jfan@mst.edu).

X.-D. Cai, C. Sui, and B. Sen are with Cisco Systems, Inc., San Jose, CA 95134 USA (e-mail: kecai@cisco.com; chsui@cisco.com; bisen@cisco.com). Color versions of one or more of the figures in this paper are available online at http://ieeexplore.ieee.org.

Digital Object Identifier 10.1109/TEMC.2019.2902070

to sacrifice more valuable space on the printed circuit board (PCB) to provide more isolation/separation in routing. Excessive crosstalk will also degrade the accuracy of post-processing in SI performance quantification such as de-embedding [1], [2] and PCB material characterization [3], [4]. A more comprehensive crosstalk analysis is required to take frequency-dependent dielectric loss and conductor loss into account.

The crosstalk generation mechanism was presented in [5] and [6], and the classic analytical crosstalk estimation formulas were derived by solving Telegrapher's equations. The classic formulas inspired many crosstalk mitigation designs by providing more isolation [7]-[13] or balancing inductive and capacitive coupling [14]–[17]. However, the classic formulas are based on the assumptions of the lossless transmission line and perfectly matched terminals, which limits their usage in a practical transmission line design. A recent study [18] presented that FEXT is not solely contributed by forward traveling crosstalk. If mismatched terminals are introduced, a combined effect due to backward traveling crosstalk and reflections at near-end and far-end mismatched terminals also contributes to FEXT. Such an effect may be negligible for coupled microstrips but is dominating for striplines, especially with a homogeneous dielectric medium. Hence, FEXT is neither independent of mismatched terminals nor equal to forward traveling crosstalk alone for practical transmission lines with impedance mismatched terminals.

Further, it was commonly believed that the forward traveling crosstalk is mainly attenuated by the lossy material. Thus, the FEXT calculated using the lossless material assumption should be a conservative estimation, which provides an upper bound crosstalk noise. But, according to our investigations, this is not necessarily true. An important phenomenon is observed that lossy conductor could increase FEXT under certain conditions. According to the simulation results shown in Fig. 1, FEXT on tightly coupled striplines increases from 0.0 to 12.0 mV after a lossy conductor is introduced.

The paper is going to follow the idea of [18] to provide a more comprehensive crosstalk analysis to demonstrate the influence of lossy dielectric and conductor for practical transmission line design. The classic crosstalk estimation formula, which is derived under lossless assumptions, will be replaced based on the proposed modal analysis [21]. In this approach, forward traveling crosstalk is a function of the superposition of received odd

0018-9375 © 2019 IEEE. Personal use is permitted, but republication/redistribution requires IEEE permission. See https://www.ieee.org/publications/rights/index.html for more information.

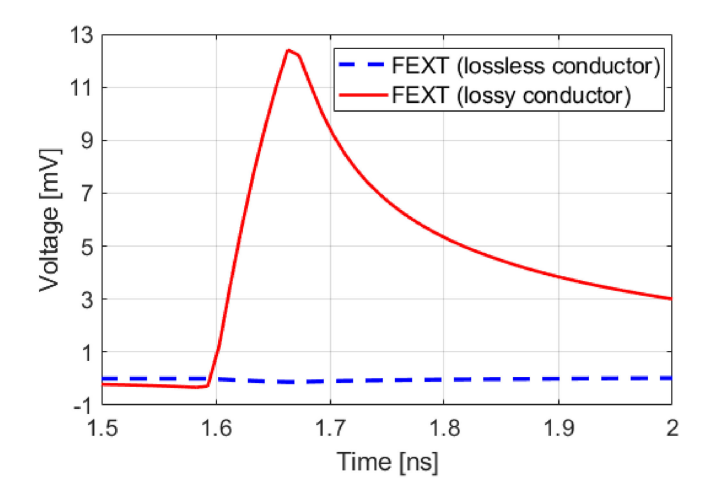


Fig. 1. FEXT for two coupled striplines simulated using the Keysight ADS Transient solver [19]. Trace width w=4.5 mils, edge-edge spacing s=3.6 mils, trace thickness t=0.7 mils, the distances between the bottom of signal traces to the upper and lower ground are $h_1=5.6$ mils and $h_2=4.9$ mils, and length =10 in. Dielectric constant (DK) is 3.6, and dissipation factor (DF) is 0.006 at 1 GHz; causal Djordjevich approximation [20] is used to model the dielectric. For the lossless conductor case, conductivity $\sigma=5.8\times10^{50}$ S/m. For the lossy conductor case, $\sigma=5.8\times10^{7}$ S/m. The incident signal has a magnitude of 1 V and rise time of 70 ps. All ports are well-matched.

mode and even mode signals, so the impact of resistance and dielectric loss tangents to FEXT can be investigated using the low-loss transmission line theories.

As the title of this paper mentioned, both comprehensiveness and practicability are considered. The comprehensiveness is defined as taking microstrips, striplines, and a lossy dielectric and conductor into account (the influence of mismatched terminals was discussed in [18]). The definition of practicability is that we are going to analyze and estimate FEXT in a closed-form approach based on transmission line theory. The authors would like to provide an insight into FEXT; therefore, lengthy numerical full-wave simulations will only serve as references or validations generally in this paper.

Notice that the investigations performed in this paper are based on the following assumptions.

- 1) The second-order effects caused by the coupling from the victim back to the aggressor are ignored.
- 2) Only the time span from the beginning of the pulse transition to the end of its propagation is considered.
- Only balanced and symmetrical transmission lines will be discussed.
- 4) All ports are well-matched.

As part of the paper organization, in Section II, the lossless transmission line model provides a good starting point for the discussion about FEXT. Section III presents the analytical and numerical analyses after the loss is applied. In Section IV, a new and practical FEXT estimation method is proposed.

II. FEXT ON LOSSLESS LINES

The classic forward traveling crosstalk estimation formula consisted of capacitive/inductive components is given

in [5] and [6] as

$$V_{\text{fwd}} = \frac{1}{2} \frac{l}{t_r} \left(|C_{21}| Z_0 - \frac{L_{21}}{Z_0} \right) V_1 \tag{1}$$

where V_1 is the magnitude of the aggressor signal that has a rise time of t_r , Z_0 is the characteristic impedance of both aggressor and victim lines whose length is l, and L_{21} and C_{21} are the off diagonal components of the per-unit-length (p.u.l.) L and C matrices (notice that C_{21} is a negative number). The constant 1/2 is due to the voltage division at the perfectly matched transmitter terminal. This expression is derived by solving Telegrapher's equations under the lossless assumptions. Unfortunately, after introducing conductor and dielectric loss, Telegrapher's equations are difficult to solve analytically. Equation (1) provides a good insight into crosstalk by separating contributions due to inductive and capacitive coupling. When the incident signal is positive, inductive domination $(|C_{21}|Z_0 < L_{21}/Z_0)$ causes a negative far-end crosstalk voltage and capacitive domination causes a positive voltage ($|C_{21}|Z_0 > L_{21}/Z_0$). The total forward crosstalk is the superposition of the inductive and capacitive components.

To introduce the influence due to loss, the idea of describing forward traveling crosstalk based on modal analysis is adopted [21]. After the aggressor signal is separated into even and odd modes, the far-end noise pulse is generated over the time interval between the arrival of the odd-mode signal and the arrival of the even-mode signal. After propagation, the forward traveling crosstalk is the superposition of the received even and odd mode signals on the victim line

$$V_{\text{fwd}} = V_{\text{even}}(l) + V_{\text{odd}}(l). \tag{2}$$

For lossless cases, rise time degradation is excluded, and the forward traveling crosstalk is only caused by the difference between the even and odd mode phase velocities due to inhomogeneous dielectric media. When the incident signal is positive, if the odd mode signal has faster phase velocity and arrives at the receiver end earlier, the forward traveling crosstalk voltage is negative. If the even mode signal propagates faster, the forward crosstalk voltage is positive. For the ideal homogeneous and lossless case, the forward traveling crosstalk is zero due to the same phase velocity for even and odd mode signals, which can be proven giving the important identity for homogeneous lossless media $LC = CL = \mu \varepsilon I_n$ [22], where the dielectric material is characterized by permittivity ε and permeability μ . I_n is an $n \times n$ identity matrix. L, C, and I_n are equal in size.

Under lossless assumptions, this modal analysis based crosstalk expression is equivalent to the classic formula (1). As illustrated in Fig. 2, unsaturated (i.e., not reaching the maximum possible value) forward crosstalk on lossless transmission lines can be expressed using (2) as

$$V_{\text{fwd}} = \frac{1}{2} \frac{T_{\text{odd}} - T_{\text{even}}}{t_r} V_1$$

$$= \frac{1}{2} \frac{l}{t_r} \left(\frac{1}{v_{p, \text{ odd}}} - \frac{1}{v_{p, \text{ even}}} \right) V_1$$
(3)

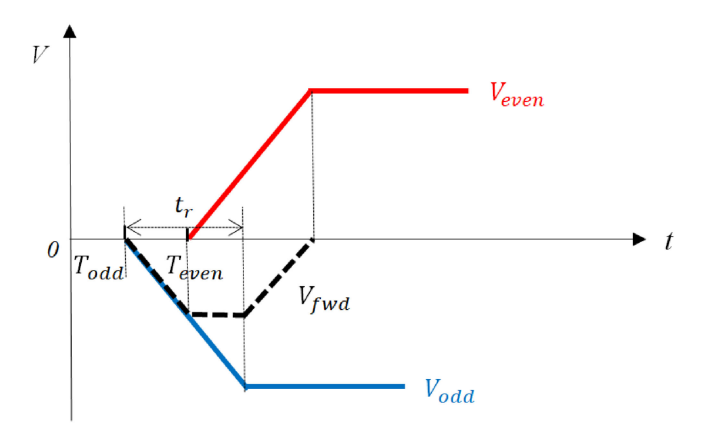


Fig. 2. Illustration of unsaturated forward crosstalk $V_{\rm fwd}$, when $v_{p, {\rm odd}} > v_{p, {\rm even}}$ on lossless transmission lines. $V_{\rm even}$ and $V_{\rm odd}$ stand for even and odd mode signals at the receiver end, respectively.

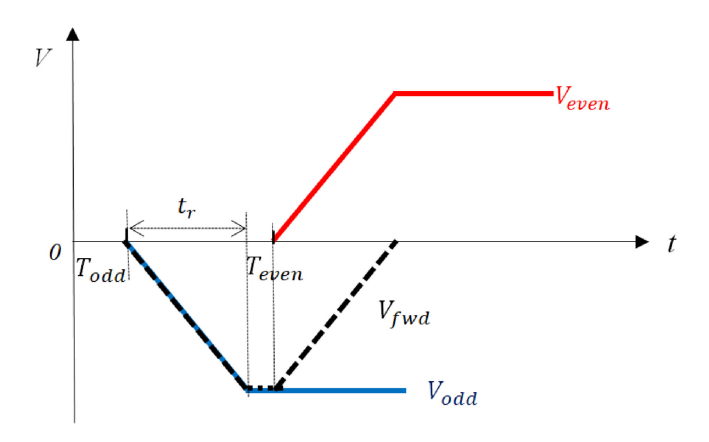


Fig. 3. Illustration of saturated forward crosstalk when $v_{p, \mathrm{odd}} > v_{p, \mathrm{even}}$ on lossless transmission lines. V_{even} and V_{odd} stand for even and odd mode signals at the receiver end, respectively.

where

$$v_{p,m} = \frac{1}{\sqrt{L_m C_m}} \tag{4}$$

$$L_m = T_v^{-1} L T_i (5)$$

$$C_m = T_i^{-1} C T_v (6)$$

$$T_v = T_i = \begin{bmatrix} \frac{1}{\sqrt{2}} & -\frac{1}{\sqrt{2}} \\ \frac{1}{\sqrt{2}} & \frac{1}{\sqrt{2}} \end{bmatrix}.$$
 (7)

Here, m represents even or odd mode. After approximating the square root in (4) by the first-order term of the Taylor series expansion, (3) approaches to (1), which means that two different expressions derived using different principles are actually describing the same forward crosstalk from different perspectives.

If the rise time is shorter than the differences between the propagation delays of the even and odd mode signals, forward crosstalk saturates. In other words,

unsaturated forward XTK,
$$T_{\rm odd} - T_{\rm even} \leq t_r$$
 saturated forward XTK, $T_{\rm odd} - T_{\rm even} > t_r$. (8)

As shown in Fig. 3, for saturated forward crosstalk, its amplitude ceases to change with transmission line length l and rise time t_r . FEXT reaches its maximum amplitude after saturation. To include the saturation case, (3) can be revised to

$$v_{\text{fwd}} = \frac{1}{2} \frac{\min(T_{\text{odd}} - T_{\text{even}}, t_r)}{t_r} v_1.$$
 (9)

For lossless striplines with homogeneous dielectric medium, forward crosstalk is always zero because $v_{p,\text{even}} = v_{p,\text{odd}}$.

In more realistic lossless striplines with an inhomogeneous dielectric material, forward crosstalk is generated due to the slightly different dielectric constants (DK) in prepreg and core layers. Cross-sectional geometry and the DK values will determine the phase velocities of the even and odd mode signals. But, normally the difference between phase velocities is too small to cause saturation. For example, for the coupled striplines illustrated in Fig. 1, if DK_{prepreg} = 3.4 and DK_{core} = 3.7, according to the results calculated by ANSYS 2D extractor (Q2D) [23], $v_{p, {\rm even}} \approx 1.58 \times 10^8 \, {\rm m/s}$ and $v_{p, {\rm odd}} \approx 1.56 \times 10^8 \, {\rm m/s}$. When $t_r = 50 \, {\rm ps}$, the striplines will not saturate unless the line length is more than 25 in, which is very long for practical fabricated PCBs.

For lossless microstrip lines, it is always true that inductive coupling is dominating ($|C_{21}|Z_0 < L_{21}/Z_0$) because air greatly reduces capacitance while inductance barely changes. Thus, negative forward crosstalk is generated for a positive incident signal on the aggressor line. The same conclusion can also be drawn by proving that the odd mode signal always has faster phase velocity ($v_{p,\text{odd}} > v_{p,\text{even}}$) using the analytical equations for two coupled microstrip lines presented in [24].

III. FEXT ON LOSSY LINES

In the previous section, the modal analysis based expression for forward crosstalk is briefly introduced. Because it is not derived using lossless assumptions like in the classic capacitive/inductive expression (1), low-loss transmission line theories can be further introduced.

We will prove that the lossy conductor can cause FEXT when even and odd mode signals are not attenuated equally. Conductor loss influenced by the proximity effect is the source of such unequal attenuation in different propagation modes. A new FEXT component due to the lossy conductor is introduced, which is shown to be important for high-speed coupled striplines such as those used in SerDes channels.

A. Low Loss Transmission Line Theories

The complex propagation constant γ is related to the p.u.l. parameters of the transmission line as follows:

$$\gamma = \sqrt{(R + j\omega L)(G + j\omega C)}.$$
 (10)

All practical transmission lines are low-loss, that is, $R \ll j\omega L$ and $G \ll j\omega C$. In this case, (10) can be approximated by the first-order term of the Taylor series expansion [25]

$$\gamma \approx j\omega\sqrt{LC}\left[1 - \frac{j}{2}\left(\frac{R}{\omega L} + \frac{G}{\omega C}\right)\right].$$
 (11)

The corresponding approximated expression for the attenuation α and phase β constants can be expressed as

$$\alpha = \frac{1}{2}R\sqrt{\frac{C}{L}} + \frac{1}{2}G\sqrt{\frac{L}{C}} = \alpha_{\rm cond} + \alpha_{\rm diel}$$
 (12)

$$\beta = \omega \sqrt{LC}.\tag{13}$$

Conductor loss is expressed as

$$\alpha_{\rm cond} = \frac{1}{2}R\sqrt{\frac{C}{L}}.$$
 (14)

The p.u.l. conductance of the mode can be related to the dielectric DF as

$$G = \tan \delta \,\omega C. \tag{15}$$

Also, the phase velocity is expressed as

$$v_p = \frac{\omega}{\beta} = \frac{1}{\sqrt{LC}}. (16)$$

Therefore, the dielectric loss can be expressed as

$$\alpha_{\rm diel} = \frac{1}{2} \tan \delta \,\omega \frac{1}{v_p}.\tag{17}$$

Equations (14) and (17) can be generalized for modal cases as

$$\alpha_{\text{diel},m} = \frac{1}{2} \tan \delta_m \omega \frac{1}{v_{p,m}}$$
 (18)

$$\alpha_{\text{cond},m} = \frac{1}{2} R_m \sqrt{\frac{C_m}{L_m}} \tag{19}$$

where the subscript m relates to a certain propagation mode. Using (18) and (19), attenuations for the even and odd mode signals will be compared. If the even and odd mode signals are attenuated equally, similar conclusions can be drawn for lossy cases as for the lossless transmission lines. However, if the attenuations are not the same, a new FEXT component appears because the received odd and even signals will then have different rise times.

B. Proximity Effect

In this section, to compare the conductor attenuations for even and odd mode signals ($\alpha_{\rm cond, even}, \alpha_{\rm cond, odd}$), investigations are performed to find the difference between the corresponding modal resistances ($R_{\rm even}, R_{\rm odd}$).

It is clear that these modal resistances are frequency dependent. First of all, this is due to the skin effect, leading to more current concentrating on the surfaces of the conductors as the frequency increases. Further, if two stripline traces are closely spaced, current distributions are affected by the interactions between the two currents, which are referred to as proximity effect [26]–[28].

As Fig. 4 illustrates, within a single stripline trace, the current spreads out near the foil surface and its density increases dramatically at the edges [29]. Fig. 5 shows that in addition to the "current dense edge" effect (or skin effect), proximity effect causes different current distributions for the even and odd mode signals. For the even mode signal, current in each conductor

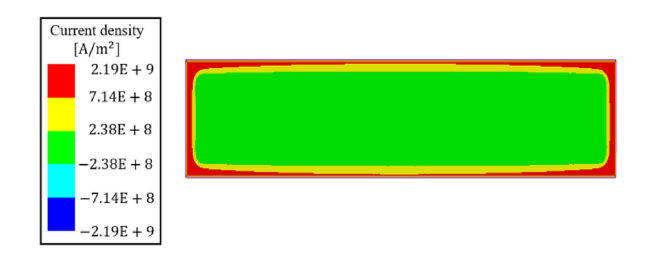


Fig. 4. Current density at 1 GHz in a single-ended rectangular stripline trace. Trace width w, trace thickness t, and dielectric heights h_1 , h_2 are shown in Fig. 6. The calculation is performed using ANSYS Q2D.

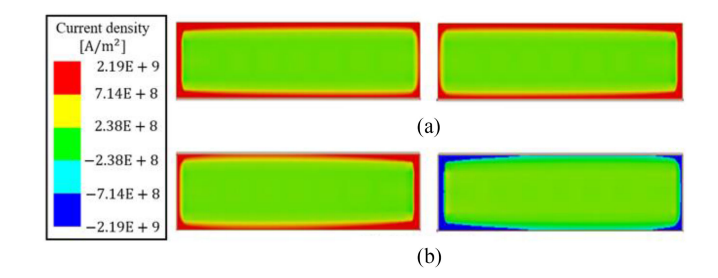


Fig. 5. Current density at 1 GHz in two strongly coupled rectangular stripline traces: (a) even mode and (b) odd mode. The geometry information of the coupled traces is shown in Fig. 6, with edge-to-edge spacing between traces s = 2 mils. The calculation is performed using ANSYS Q2D.

"rejects" each other, and distributes more sparsely as the distances getting closer. For the odd mode signal, current in each conductor "attracts" each other and tends to concentrate near the center between traces, using each other as their return loop. Such differences in current distribution lead to different modal resistances. It is worth mentioning that the higher the frequency, the stronger the proximity effect.

Modal resistances can be estimated by converting the p.u.l. resistance matrix using the transformation matrices T_i, T_v shown in (7), when the coupled traces are assumed symmetrical and reciprocal

$$R_m = T_v^{-1} R T_i$$

$$\approx \left(\begin{bmatrix} \frac{1}{\sqrt{2}} & -\frac{1}{\sqrt{2}} \\ \frac{1}{\sqrt{2}} & \frac{1}{\sqrt{2}} \end{bmatrix} \right)^{-1} \cdot \begin{bmatrix} R_{\text{self}} & R_{\text{mutual}} \\ R_{\text{mutual}} & R_{\text{self}} \end{bmatrix} \cdot \begin{bmatrix} \frac{1}{\sqrt{2}} & -\frac{1}{\sqrt{2}} \\ \frac{1}{\sqrt{2}} & \frac{1}{\sqrt{2}} \end{bmatrix}$$

$$= \begin{bmatrix} R_{\text{self}} + R_{\text{mutual}} & 0\\ 0 & R_{\text{self}} - R_{\text{mutual}} \end{bmatrix}.$$
 (20)

Thus, the even and odd mode resistances are

$$R_{\rm even} \approx R_{\rm self} + R_{\rm mutual}$$
 (21)

$$R_{\rm odd} \approx R_{\rm self} - R_{\rm mutual}.$$
 (22)

The difference between $R_{\rm odd}$ and $R_{\rm even}$ is defined as ΔR , which causes the difference between the conductor attenuations for the even and odd mode signals

$$\Delta R = R_{\rm odd} - R_{\rm even} \approx -2R_{\rm mutual}.$$
 (23)

It is clear that $R_{\rm mutual}$ leads to the differences between modal resistances. Since a general formulation of the resistance matrix taking skin effect and proximity effect into account is difficult,

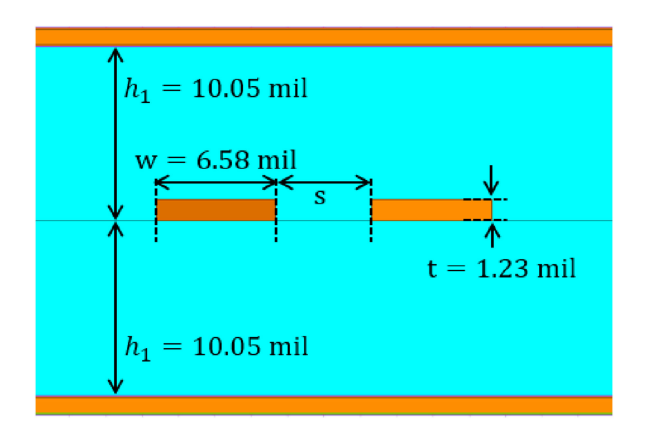


Fig. 6. Cross-sectional geometry of two coupled symmetrical stripline traces.

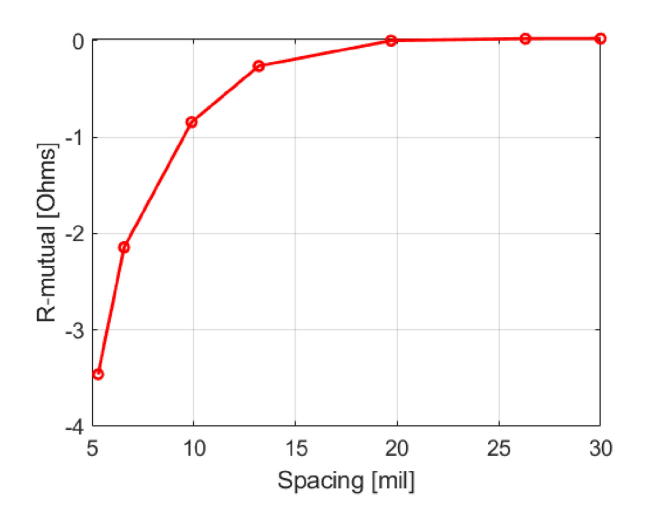


Fig. 7. Relationship between $R_{
m mutual}$ and trace spacing s at 10 GHz. The calculation is performed using ANSYS Q2D.

to demonstrate the properties of "mutual" resistance $R_{\rm mutual}$, a set of numerical simulations were carried out using ANSYS Q2D. The conductors are solved using the solve-inside mode, which creates a mesh inside the conductors. The cross-sectional geometry is shown in Fig. 6. The spacing between the two traces is swept from 5.3 to 30 mils.

As Fig. 7 shows, the stronger coupling between traces makes $R_{\rm mutual}$ negative. The value of $R_{\rm mutual}$ increases as coupling gets weaker and finally makes it a positive number. It can be observed that the changing trend stops until the proximity effect is almost negligible with the spacing reaching 26.7 mils (about four times of the trace width), and the mutual resistance converges to $0.02\,\Omega$, which is approximately equal to the resistance of the reference plane at 10 GHz. The impact of proximity effect to $R_{\rm mutual}$ is illustrated in this example, and it is obvious that $R_{\rm mutual}$ is sensitive to the coupling between two traces.

The frequency dependence of $R_{\rm mutual}$ is shown in Fig. 8. As frequency goes higher, the influence of the proximity effect is getting more dominant. The difference between $R_{\rm even}$ and $R_{\rm odd}$ is shown in another format using the ratio between $R_{\rm even}$ and $R_{\rm odd}$ in Fig. 9. For the strongly coupled case with s=5.3 mils, $R_{\rm odd}$ is 6%–12% larger than $R_{\rm even}$ from approximately 2 to

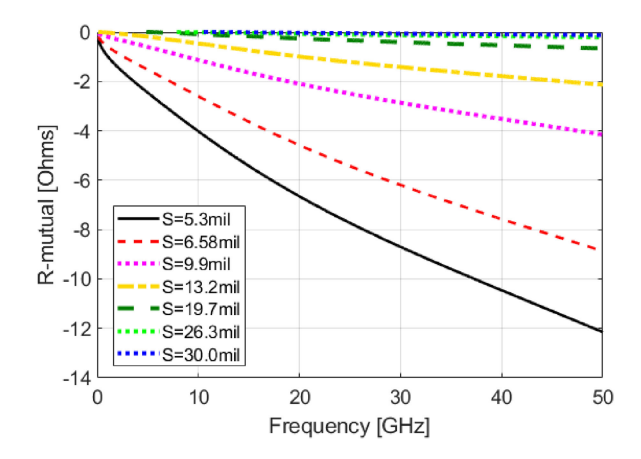


Fig. 8. Frequency-dependence of $R_{\rm mutual}$ is for striplines with different trace spacing. The calculation is performed using ANSYS Q2D.

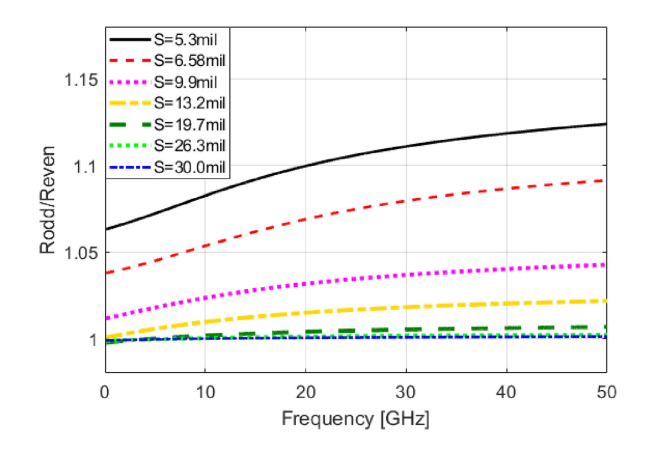


Fig. 9. Ratio between the odd and even mode resistances $(R_{\rm odd}/R_{\rm even})$ as a function of frequency and trace spacing. The calculation is performed using ANSYS Q2D.

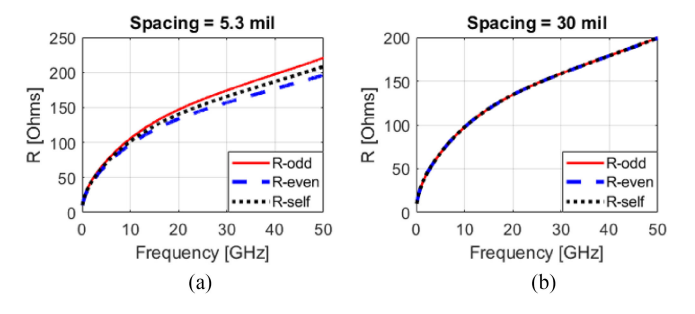


Fig. 10. Comparison between $R_{\rm odd}$, $R_{\rm even}$, and $R_{\rm self}$ for (a) s=5.3 mils and (b) s=30.0 mils.

50 GHz. For weakly coupled cases with $s \ge 26.3$ mils, $R_{\rm odd}$ is approximately equal to $R_{\rm even}$.

It can be observed that for strongly coupled traces $R_{\rm mutual}$ becomes negative. Thus, according to (21) and (22), we have $R_{\rm odd} > R_{\rm self} > R_{\rm even}$. At the same time, the differences between $R_{\rm odd}$, $R_{\rm self}$, and $R_{\rm even}$ become negligible for weakly coupled traces (see Fig. 10). Such negative $R_{\rm mutual}$ is also presented by [30, Figs. 5 and 7], calculated using a modified model based on the finite element method. In addition, there is experimental evidence that $R_{\rm mutual}$ between two conductors can be

negative for high enough frequency in [31, Fig. 4]. According to [32], the negative $R_{\rm mutual}$ is possible as long as the total power dissipated is positive (a passive conductor cannot generate power), namely, $|R_{\rm mutual}| < R_{\rm self}$.

A hypothesis is brought up by the author that $R_{\rm mutual}$ is contributed by the reference plane resistance and proximity effect. The reference plane resistance is positive, and numerically negligible to $R_{\rm self}$ due to widely distributed current on the reference plane. Proximity effect's contribution is negative and very sensitive to frequency and the separation between traces. Thus, as frequency goes up, for strongly coupled traces the majority of $R_{\rm mutual}$ is contributed by proximity effect, which makes $R_{\rm mutual}$ no longer negligible to $R_{\rm self}$. According to (21) and (22), the negative $R_{\rm mutual}$ makes $R_{\rm odd} > R_{\rm even}$ and the differences between $R_{\rm odd}$ and $R_{\rm even}$ is going to become larger with increasing frequency and narrower spacing between traces.

To sum up, for weakly coupled traces, the even and odd modes have nearly equal resistances $(R_{\rm odd} \approx R_{\rm even})$ because $R_{\rm mutual}$ is negligible. As the coupling gets stronger, $R_{\rm mutual}$ becomes negative, and its absolute value increases, which makes $R_{\rm odd} > R_{\rm even}$. It is the proximity effect that results in the difference in the modal conductor attenuations, and the higher the frequency, the larger the difference.

C. Striplines With a Lossy Homogeneous Dielectric Material and a Lossy Conductor

For striplines with a perfectly homogenous dielectric medium, the even- and odd-mode dielectric loss-tangent values are the same, $\tan\delta_{\rm even} = \tan\delta_{\rm odd} = \tan\delta$. The modal phase velocities are also equal, i.e., $v_{p,\rm even} = v_{p,\rm odd}$. So, according to (18), the dielectric losses are also equal ($\alpha_{\rm diel,even} = \alpha_{\rm diel,odd}$).

The modal conductor losses can be calculated using (19). It is easy to prove that $\sqrt{C_{\rm odd}/L_{\rm odd}} > \sqrt{C_{\rm even}/L_{\rm even}}$. Indeed,

$$\sqrt{\frac{C_{\text{odd}}}{L_{\text{odd}}}} = \sqrt{\frac{C_{11} + |C_{21}|}{L_{11} - L_{21}}} > \sqrt{\frac{C_{11} - |C_{21}|}{L_{11} + L_{21}}} = \sqrt{\frac{C_{\text{even}}}{L_{\text{even}}}}.$$
(24)

For tightly coupled cases with non-PEC conductors, the strong proximity effect leads to $R_{\rm odd} > R_{\rm even}$. Together with (24), it is obvious that $\alpha_{\rm cond.odd} > \alpha_{\rm cond.even}$.

Thus, for lossy striplines with a homogeneous dielectric material, the dielectric loss attenuates the even and odd mode signals equally, while conductor loss attenuates the odd mode signal more than the even mode signal. This difference in attenuations leads to different rise times in the even and odd mode signals at the receiver end, which further results in a new FEXT component. We define it as the FEXT due to the lossy conductor.

The phenomenon can be verified using Keysight ADS. Using the same striplines studied in Fig. 1, the received even and flipped odd mode signals at the victim receiver with lossless conductors are shown in Fig. 11. Rise time degradation can be observed when a lossy conductor is introduced by comparing Fig. 11 with Fig. 12(a). In the case with the lossy conductors, the received odd mode signal, when flipped in polarity, no longer overlaps with the received even mode signal, like in the lossless conductor case, because of the different conductor

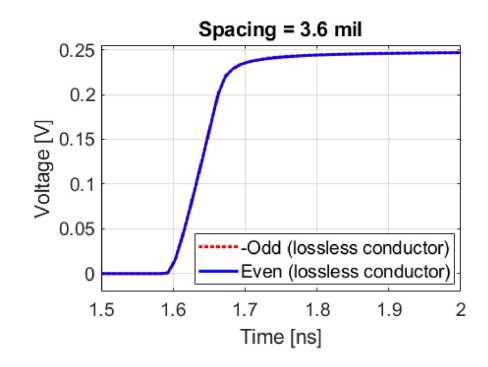


Fig. 11. Received even and odd (flipped for easier comparison) mode signals for the stripline with s=3.6 mil and lossless conductors.

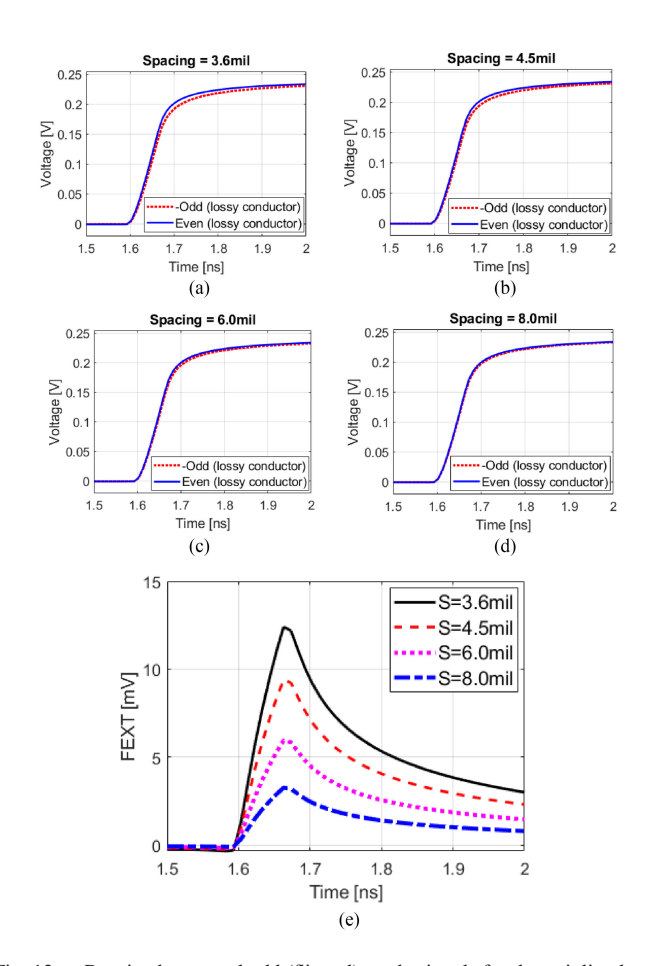


Fig. 12. Received even and odd (flipped) mode signals for the stripline lossy conductors when spacing is set to (a) 3.6, (b) 4.5, (c) 6.0, and (d) 8.0 mils. In (e), the resulting FEXT values are compared, which are the superposition of the received even and odd mode signals.

attenuations in the even and odd mode signals due to the proximity effect. In Fig. 12(a), such difference in the conductor attenuations causes the odd and the even mode signals to have approximately 0.25 and 0.20 ns rise times (defined as 10%-90%), respectively. The difference between the rise time is about 0.05 ns, which leads to a 12 mV FEXT peak, as shown in Fig. 1.

Three additional simulations are performed by increasing the trace spacing to 4.5/6.0/8.0 mils. As shown in Fig. 12(a)–(d), the difference between the received even mode signal and flipped



Fig. 13. Test board having two coupled striplines with different lengths.

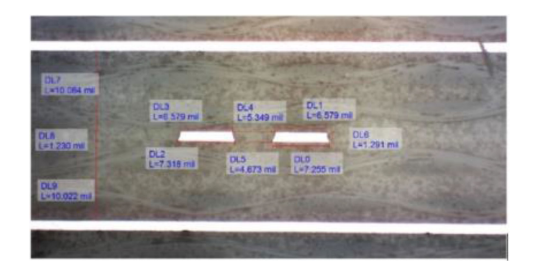


Fig. 14. Cross section of the coupled striplines. The edge-to-edge spacing *s* between traces is approximately equal to 4.7 mils. Other geometry information is illustrated in Fig. 6.

odd mode signal gets smaller with the increase of the trace spacing because of weaker proximity effect. The decreasing FEXT can be clearly observed in Fig. 12(e). When spacing s=8.0 mils, the odd mode signal and the even mode signal have 10%-90% rise time of approximately equal to 0.21 and 0.19 ns, respectively. When compared to the case of s=3.6 mils, the difference between the rise time decreases from 0.05 to 0.02 ns, which makes the FEXT peak to decrease from 12 to 3 mV.

To further validate the proposed theory with measurements, a test vehicle containing multiple differential stripline pairs was fabricated, as shown in Fig. 13. Two lengths (1.3 and 10.8 in) were used for VNA measurements and an in-house 2X-Thru de-embedding approach named SFD was applied to remove the connector and launching effects [33]–[35]. The cross-sectional geometry of the coupled lines and their foil roughness levels are obtained from the two-dimensional (2D) cross-sectional measurements with the obtained picture shown in Fig. 14. The effective DK and $\tan \delta$ are extracted using the method proposed in [36], assuming a homogeneous dielectric medium.

Traditionally, FEXT is estimated under the lossless conductor assumption. Thus, a Q2D model is studied first with practically infinite conductivity of $\sigma=5.8\times10^{50}~\mathrm{S/m}$. Then, another Q2D model is investigated with $\sigma=5.8\times10^{7}~\mathrm{S/m}$. Both models use the same frequency-dependent DK and DF described by the intrinsically causal Djordjevic model, with DK = $3.4~\mathrm{and}~\mathrm{DF}=0.0034~\mathrm{at}~1~\mathrm{GHz}$. Modeled S-parameters calculated by Q2D are exported to compare with the VNA measurement results. It is also worth mentioning that the trapezoidal shape of the traces (due to an etching angle) should be measured and modeled in Q2D to capture proximity effect accurately.

The comparison in the frequency-domain FEXT ($|S_{41}|$) between the two models and measurement is shown in Fig. 15. The ports are defined at the ends of de-embedded transmission lines with the resulting length equal to $10.8-1.29=9.51\,\mathrm{in}$. It is clear that the model using lossy conductors has a better match with the measurement data, and the resulting FEXT magnitude ($|S_{41}|$) is around $-25\,\mathrm{dB}$ in the frequency band from

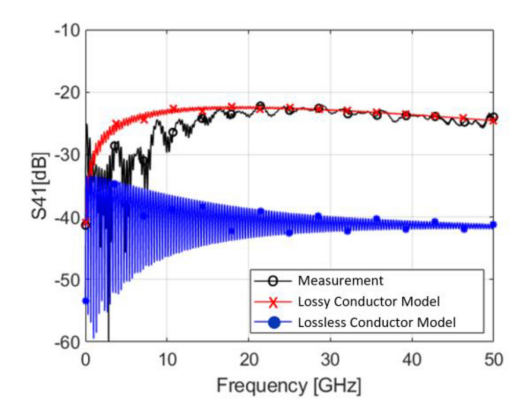


Fig. 15. Comparison of the frequency-domain FEXT $(|S_{41}|)$ between measurement and Q2D models assuming homogeneous dielectric material.

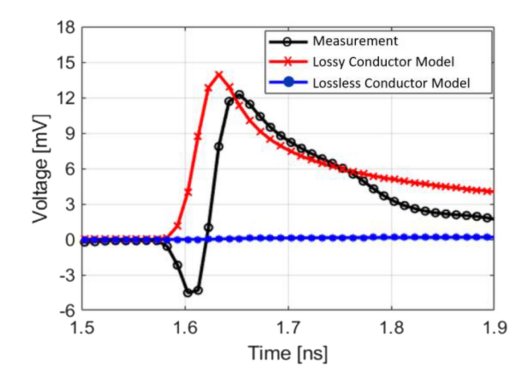


Fig. 16. Comparison of the time-domain FEXT between measurement and Q2D models assuming a homogeneous dielectric material. The waveforms are calculated by importing the corresponding *S*-parameters into the Keysight ADS Transient solver.

approximately 10 to 50 GHz. The Q2D model using lossless conductors results in $|S_{41}|$ below -35 dB generally, which greatly underestimates the FEXT on coupled striplines. Thus, as demonstrated, estimating FEXT on coupled striplines under the lossless conductor assumption may not be accurate and useful. The same conclusion can be drawn from the comparison in the time domain, as shown in Fig. 16. The model with lossy conductors provides much better FEXT estimation.

Notice that the measurement has a dip at 1.6 ns, which is not shown in the lossy conductor mode. That is due to the slight inhomogeneity between the core and prepreg in the fabricated PCB. Such inhomogeneity is making the odd mode signal having a faster phase velocity. A negative FEXT due to different phase velocity is generated as a result. Also, the dielectric material will not attenuate even and odd mode signals equally according to (18). Thus, for well-matched fabricated lossy striplines with non-ideal homogenous dielectric, the total FEXT is contributed by three components shown in Table I.

D. Lossy Microstrips

For coupled microstrips with an inhomogeneous dielectric material, $v_{p, \mathrm{even}} \neq v_{p, \mathrm{odd}}$. Also, the even and odd DFs are no longer equal: $\tan \delta_{\mathrm{even}} \neq \tan \delta_{\mathrm{odd}}$; hence, we do not know whether $\alpha_{\mathrm{diel, even}}$ and $\alpha_{\mathrm{diel, odd}}$ are equal or not. The proximity

TABLE I FEXT CONTRIBUTORS AND PEAK POLARITY

| FEXT Contributors | Polarity |
|--|--|
| Different phase velocity due to inhomogeneity | Positive when $v_{p,even} > v_{p,odd}$ Negative when $v_{p,even} < v_{p,odd}$ |
| Different conductor losses for even and odd mode signal | Always positive because $\alpha_{cond,odd} > \alpha_{cond,even}$ |
| Different dielectric losses for even and odd mode signal | Positive when $\alpha_{diel,odd} > \alpha_{diel,even}$ Negative when $\alpha_{diel,odd} < \alpha_{diel,even}$ |

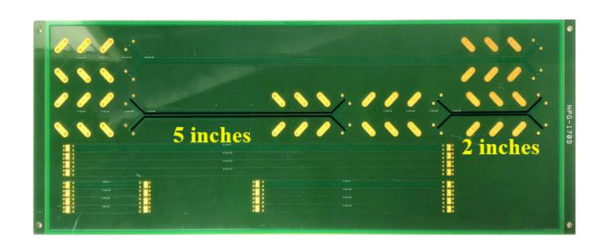


Fig. 17. Testing board has two coupled microstrips with different lengths: 2 and 5 in. Trace width w=5 mil, edge-to-edge spacing s=11 mils, trace thickness t=1.4 mils, the dielectric height h=2.5 mils. At 1 GHz, dielectric constant (DK) is 3.8 and dissipation factor (DF) is 0.02.

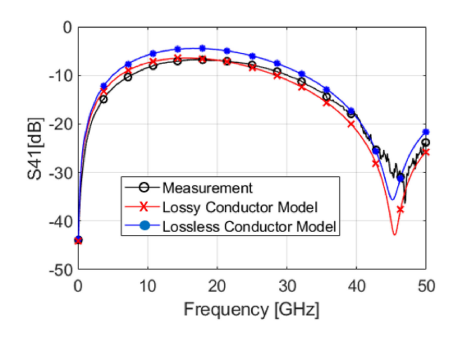


Fig. 18. Frequency-domain (S_{41}) FEXT comparison between measurement and Q2D models and using lossy and lossless conductor.

effect still exists. Thus, the total FEXT on well-matched lossy microstrips is also contributed by the three factors shown in Table I.

A testing coupon containing multiple differential microstrip pairs was fabricated for validation (see Fig. 17). Two of the microstrips (2.0 and 5.0 in) were used for measurement and deembedding. The geometry and material information are obtained from the PCB layout file. The model using lossless conductor will be compared with the one generated using a lossy conductor. According to Fig. 18, in the frequency domain, the difference between two models are small. Both models match with the measurement data. The time-domain comparison is illustrated in Fig. 19; the model with the lossy conductor has a good match with the measurement data, while conservative FEXT estimation can be obtained from the model under lossless assumptions, which is still useful for a practical design.

Thus, for coupled microstrips the contribution from different phase velocity due to inhomogeneous dielectric is still dominat-

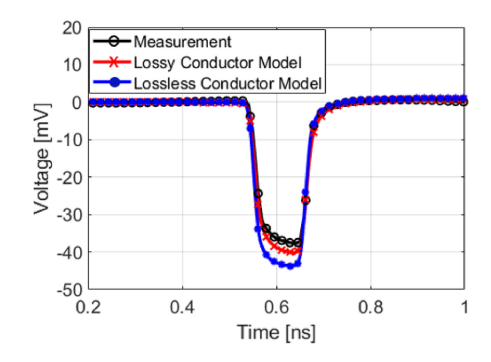


Fig. 19. Time-domain FEXT comparison between Q2D models using lossy and lossless conductor. The waveforms are calculated by importing *S*-parameters calculated by Q2D into the Keysight ADS Transient solver.

ing, even if received signal's rise time is changed a little bit by the lossy material. According to p.u.l. parameters calculated by Q2D, the odd mode signal has faster phase velocity and arrives at the far-end terminal about 0.1 ns earlier than the even mode signal, causing FEXT due to inhomogeneity with negative polarity. The odd mode signal is attenuated more than the even mode signal ($\alpha_{\rm odd} > \alpha_{\rm even}$); thus, FEXT due to the lossy conductor and dielectric with positive polarity is generated. The opposite polarities of FEXT components due to dielectric and conductor cause lossy conductor model to produce smaller FEXT compared to the lossless conductor case.

Therefore, for lossy microstrips, estimating FEXT using lossless assumptions is still accurate enough practically. The impact of lossy dielectric material and conductor is almost negligible.

IV. FEXT ESTIMATION METHODOLOGY

To estimate the impact of lossy material to FEXT fast and practically, a new FEXT estimation methodology is developed using several rules of thumb without calculating *S*-parameters in a full-wave simulation tool.

As we know, the attenuation of the channel goes up with frequency, a simple and practical way to approximate the frequency-dependent loss is to apply a one-pole RC low pass filter [21], [37]. With known even or odd signal input $v_m^{\rm in}(t)$, the step response is expressed with the following estimation:

$$\frac{v_m^{\text{out}}}{v_m^{\text{in}}} = 1 - e^{-\frac{t_m}{\tau_m}} \tag{25}$$

where $v_m^{\rm out}$ is the output voltage, and m stands for the even or odd mode. If the rise times are defined with the 10% and 90% voltage magnitude points, the time constant required to degrade a step to a specific 10%–90% rise time can be calculated as

$$tr_m^{\text{out}}\big|_{10\%-90\%} = t_{m,90\%} - t_{m,10\%}$$

= $2.3\tau_m - 0.105\tau_m = 2.195\tau_m$. (26)

Notice that $t_{m,90\%}$ and $t_{m,10\%}$ are determined by (25), with $v_m^{\rm out}/v_m^{\rm in}$ set to 0.9 and 0.1. The time constant for the one-pole filter is expressed as

$$\tau_m = \frac{tr_m^{\text{out}}|_{10\% - 90\%}}{2.195}.$$
 (27)

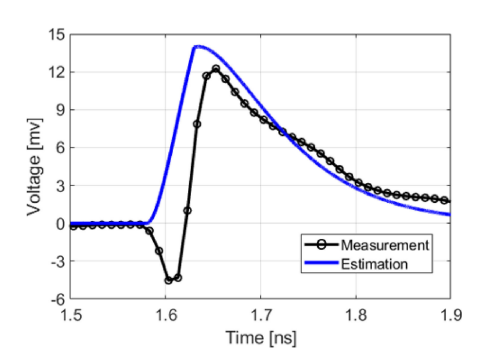


Fig. 20. Comparison of the time-domain FEXT between measurement and estimation assuming a homogeneous dielectric material. The geometry and material information are shown in Figs. 6 and 14.

A rough approximation assuming the shape of the rising edge is Gaussian can be applied to estimate the output rise time [37]

$$tr_m^{\text{out}}\big|_{10\%-90\%} = \sqrt{tr_{\text{in}}^2 + \left(tr_m^{10\%-90\%}\right)^2}.$$
 (28)

The intrinsic rise time $tr_{\rm in}$ is known, and the intrinsic interconnect rise time $tr_m^{10\%-90\%}$ can be approximated using the 3-dB bandwidth of the one-pole filter [21]

$$tr_m^{10\%-90\%} = \frac{0.35}{f_m^{3\,\text{dB}}}.$$
 (29)

Using p.u.l. matrix calculated using analytical equations or a 2-D solver, the attenuation factor can be calculated using (12), and expressed as a frequency-dependent function $\alpha_m(f)$. The line length (l) is known. Thus, $f_m^{3\,\mathrm{dB}}$ can be obtained by solving the following equation:

$$\alpha_m \left(f_m^{3 \, \mathrm{dB}} \right) = \frac{3 \, [\mathrm{dB}]}{8.686 \, [\mathrm{dB/Np}] \cdot l \, [\mathrm{m}]}. \tag{30}$$

The output modal waveform can be calculated using $v_m^{\rm out}(t)=(1-e^{-\frac{t_m}{r_m}})v_m^{\rm in}(t)$, according to (25). The estimated waveform of FEXT is the superposition of the received even and odd mode signals

$$FEXT_{est}(t) = v_{even}^{out}(t) + v_{odd}^{out}(t).$$
 (31)

Another estimated FEXT can be obtained using 20%–80% rise time, which gives smaller FEXT when compared to the results estimated using 10%–90% rise time. As a rule of thumb, we use the mean value of two estimated FEXT voltage as the final estimation result. The estimated FEXT waveform FEXT $_{\rm est}(t)$ can be calculated, and the maximum value of FEXT $_{\rm est}(t)$ is the estimated FEXT peak.

To verify the proposed estimation method, coupled striplines on the fabricated testing board shown in Fig. 13 are used. The p.u.l. matrices calculated by Q2D are used as the inputs of the estimation methodology. The comparison between estimated and measured FEXT is shown in Fig. 20. It can be observed that even if there are some differences between the estimated and measured FEXT waveforms, the estimation error is acceptable (about 15%) at the FEXT peak.

TABLE II
TRANSMISSION LINES WITH LOSSY DIELECTRIC AND CONDUCTOR

| Line types | FEXT contributors |
|--|--|
| Lossy Microstrips | Different phase velocity due to inhomogeneity (dominating) Different conductor losses for even and odd mode signal Different dielectric losses for even and odd mode signal Mismatched terminals |
| Lossy striplines (ideal homogeneous dielectric material) | Mismatched terminals Different conductor losses for even and odd mode signal |
| Lossy striplines (slightly inhomogeneous dielectric material) | Mismatched terminals Different phase velocities due to inhomogeneity Different conductor losses for even and odd mode signal Different dielectric losses for even and odd mode signal |

V. CONCLUSION

This paper provides a comprehensive analysis for crosstalk including the effects of a lossy conductor and dielectric material, which are often neglected. The increase of the FEXT in striplines due to lossy conductors was analyzed. To further explore such a phenomenon, a modal analysis based description of forward crosstalk was introduced. According to our analytical and numerical investigations, we found that the proximity effect due to lossy conductors causes different attenuations for even and odd modes, and FEXT was generated by the superposition of the received even and odd mode signals with different rise times. We defined a new concept called FEXT-due-to-lossy-conductors, and it plays a significant role in high-speed striplines. In addition, a practical and fast FEXT estimation approach was proposed with closed-form formulas that can be easily adopted in high-speed design practice. Following the approach provided in this paper, a good accuracy was achieved without resorting to lengthy numerical calculations. In the end, a summary table for different transmission line types with lossy dielectric material and conductor and their FEXT contributors is listed in Table II.

Notice that the conclusion shown in [18] for lines with approximately 10% mismatched terminals are also included in Table II. For coupled microstrips, the different phase velocity is the dominating FEXT contributor. The conventional FEXT estimation approach expressed as (1) may provide results with acceptable accuracy. For lossy coupled striplines, all the FEXT contributors listed in the table have comparable impact. Thus, neglecting any factors could lead to large FEXT estimation error.

REFERENCES

- B. Chen et al., "Analytical and numerical sensitivity analyses of fixtures de-embedding," in Proc. IEEE Int. Symp. Electromagn. Compat., Ottawa, ON, Canada, 2016, pp. 440–444.
- [2] L. Ye et al., "Thru-reflect-line calibration technique: Error analysis for characteristic impedance variations in the line standards," *IEEE Trans. Electromagn. Compat.*, vol. 59, no. 2, pp. 779–788, Jun. 2017.

- [3] S. Jin, X. Fang, B. Chen, H. Gao, X. Ye, and J. Fan, "Validating the transmission-line based material property extraction procedure including surface roughness for multilayer PCBs using simulations," in *Proc. IEEE Int. Symp. Electromagn. Compat.*, Ottawa, ON, Canada, 2016, pp. 472– 477.
- [4] S. Jin, B. Chen, X. Fang, H. Gao, X. Ye, and J. Fan, "Improved "Root-Omega" method for transmission-line-based material property extraction for multilayer PCBs," *IEEE Trans. Electromagn. Compat.*, vol. 59, no. 4, pp. 1356–1367, Aug. 2017.
- [5] D. B. Jarvis, "The effects of interconnections on high-speed logic circuit," IEEE Trans. Electron. Comput., vol. EC-12, no. 5, pp. 476–487, Oct. 1963.
- [6] J. E. Bracken, "Improved formulas for crosstalk coefficients," in *Proc. DesignCon*, 2016.
- [7] B. Chen et al., "Integrated crosstalk noise (ICN) analysis among multiple differential BGA and via pairs by using design of experiments (DoE) method," in Proc. IEEE Int. Symp. Electromagn. Compat., Washington, DC, USA, 2017, pp. 112–117.
- [8] F. D. Mbairi, W. P. Siebert, and H. Hesselbom, "High-frequency transmission lines crosstalk reduction using spacing rules," *IEEE Trans. Compon. Packag. Technol.*, vol. 31, no. 3, pp. 601–610, Sep. 2008.
- [9] G. Shiue, C. Chao, and R. Wu, "Guard trace design for improvement on transient waveforms and eye diagrams of serpentine delay lines," *IEEE Trans. Adv. Packag.*, vol. 33, no. 4, pp. 1051–1060, Nov. 2010.
- [10] Y.-S. Cheng, W.-D. Guo, C.-P. Hung, R.-B. Wu, and D. D. Zutter, "Enhanced microstrip guard trace for ringing noise suppression using a dielectric superstrate," *IEEE Trans. Adv. Packag.*, vol. 33, no. 4, pp. 961–968, Nov. 2010.
- [11] K. Lee, H.-B. Lee, H.-K. Jung, J.-Y. Sim, and H.-J. Park, "A serpentine guard trace to reduce the far-end crosstalk voltage and the crosstalk induced jitter of parallel microstrip lines," *IEEE Trans. Adv. Packag.*, vol. 31, no. 4, pp. 809–817, Nov. 2008.
- [12] R.-B. Sun, C.-Y. Wen, and R.-B. Wu, "A new isolation structure of pogo pins for crosstalk reduction in a test socket," *IEEE Trans. Compon. Packag. Technol.*, vol. 1, no. 4, pp. 586–594, Apr. 2011.
- [13] Y.-S. Li, Y.-L. Xu, D.-C. Yang, J. Li, X.-C. Wei, and E.-P. Li, "A shield-ing structure for crosstalk reduction in silicon interposer," *IEEE Microw. Wireless Compon. Lett.*, vol. 26, no. 4, pp. 246–248, Apr. 2016.
- [14] P. Muthana and H. Kroger, "Behavior of short pulses on tightly coupled microstrip lines and reduction of crosstalk by using overlying dielectric," *IEEE Trans. Adv. Packag.*, vol. 30, no. 2, pp. 511–520, Aug. 2007.
- [15] W. Jiang, X. Cai, B. Sen, and G. Wang, "Equation-based solutions to coupled, asymmetrical, lossy, and nonuniform microstrip lines for tabrouting applications," *IEEE Trans. Electromagn. Compat.*, vol. 61, no. 2, pp. 548–557, Apr. 2019.
- [16] R. K. Kunze, Y. Chu, Z. Yu, S. K. Chhay, M. Lai, and Y. Zhu, "Crosstalk mitigation and impedance management using tabbed lines," Intel White Paper, 2015.
- [17] B. Chen et al., "Differential integrated crosstalk noise (ICN) mitigation in the pin field area of Serdes channel," in Proc. IEEE Int. Symp. Electromagn. Compat., Long Beach, CA, USA, 2018, pp. 533–537.
- [18] S. Yong, K. Cai, B. Sen, J. Fan, V. Khilkevich, and C. Sui, "A comprehensive and practical way to look at crosstalk for transmission lines with mismatched terminals," in *Proc. IEEE Int. Symp. Electromagn. Compat.*, Long Beach, CA, USA, 2018, pp. 538–543.
- [19] Keysight Technologies, Inc., Advanced Design System (ADS) Documentation (2016 release), Santa Rosa, CA, USA, 2016.
- [20] A. R. Djordjevic, R. M. Biljic, V. D. Likar-Smiljanic, and T. K. Sarkar, "Wideband frequency-domain characterization of FR-4 and time-domain causality," *IEEE Trans. Electromag. Compat.*, vol. 43, no. 4, pp. 662–667, Nov. 2001.
- [21] S. H. Hall and H. L. Heck, *Advanced Signal Integrity for High-Speed Digital Designs*. Hoboken, NJ, USA: Wiley.
- [22] C. R. Paul. Analysis of Multiconductor Transmission Lines, 2nd ed. Hoboken, NJ, USA: Wiley, p. 478
- [23] ANSYS, Inc., ANSYS Electronics Desktop Online Help 2D Extractor (2018 release), Canonsburg, PA, USA, 2018.
- [24] R. Garg and I. J. Bahl, "Characteristics of coupled microstriplines," *IEEE Trans. Microw. Theory Techn.*, vol. 27, no. 7, pp. 700–705, Jul. 1979
- [25] D. M. Pozar, Microwave Engineering, 4th ed. Hoboken, NJ, USA: Wiley. p. 79.
- [26] H.A. Wheeler, "Formulas for the skin effect," *Proc. IRE*, vol. 30, no. 9, pp. 412–424, Sep. 1942.
- [27] M.E. Hellman and I. Palocz, "The effect of neighboring conductors on the currents and fields in plane parallel transmission lines," *IEEE Trans. Microw. Theory Techn.*, vol. 17, no. 5, pp. 254–259, May 1969.

- [28] G. Smith, The Proximity Effect in Systems of Parallel Conductors and Electrically Small Multiturn Loop Antennas. Fort Belvoir, VA, USA: Defense Tech. Inf. Center, 1971.
- [29] R. E. Collin, Foundation for Microwave Engineering, 2nd ed. New York, NY, USA: McGraw-Hill, 1992.
- [30] S. H. You and E. F. Kuester, "Fast and direct coupled-microstrip interconnect reduced-order modeling based on the finite-element method," *IEEE Trans. Microw. Theory Tech.*, vol. 54, no. 5, pp. 2232–2242, May 2006
- [31] D. F. Williams, J. E. Rogers, and C. L. Holloway, "Multiconductor transmission-line characterization: Representations, approximations, and accuracy," *IEEE Trans. Microw. Theory Tech.*, vol. 47, no. 4, pp. 403–409, Apr. 1999.
- [32] J. E. Bracken, Mutual Resistance in Spicelink. Pittsburgh, PA, USA: Ansoft Corp., 2000
- [33] Y. Chen et al., "Signal-signal D-probe and unified launch pads designs," IEEE Electromagn. Compat. Mag., vol. 7, no. 3, pp. 101–106, Oct.–Dec. 2018.
- [34] B. Chen et al., "8-Port network de-embedding by using SFD," in Proc. IEEE Int. Symp. Electromagn. Compat., Long Beach, CA, USA, 2018, pp. 52–56.
- [35] Y. Chen, B. Chen, R. Zai, and J. Drewniak, "De-embedding comparisons of 1X-Thru SFD, 1-Port AFR, and 2X-Thru SFD," in *Proc. IEEE Int. Asia-Pacific Symp. Electromagn. Compat.*, Singapore, 2018. pp. 160–164.
- [36] S. Yong et al., "Dielectric dissipation factor (DF) extraction based on differential measurements and 2-D cross-sectional analysis," in Proc. IEEE Int. Symp. Electromagn. Compat., Long Beach, CA, USA, 2018, pp. 217–222.
- [37] E. Bogatin, Signal and Power Integrity Simplified, 2nd ed. Englewood Cliffs, NJ, USA: Prentice-Hall, 2009.



Shaohui Yong (S'17) received the B.S. degree in electrical engineering from Beijing Jiaotong University, Beijing, China, in 2013. He is currently working toward the Ph.D. degree in electrical engineering at the EMC Laboratory, Missouri University of Science and Technology (formerly University of Missouri – Rolla), Rolla, MO, USA.

His research interests include signal integrity in high-speed digital systems, electromagnetic interference, and electrostatic discharge.



Victor Khilkevich (M'08) received the Ph.D. degree in electrical engineering from Moscow Power Engineering Institute, Technical University, Moscow, Russia, in 2001.

He is currently an Assistant Professor with the Missouri University of Science and Technology, Rolla, MO, USA. His research interests include microwave imaging, automotive electromagnetic compatibility modeling, and high-frequency measurement techniques.

Xiao-Ding Cai (M'00) received the Ph.D. degree in electrical engineering from the University of Ottawa, Ottawa, ON, Canada.

He has been a High-speed Signal Integrity Engineer assuming different responsibilities for Nortel Networks, Sun Microsystems, Juniper Networks, Rambus, and Cisco Systems.



Chunchun Sui (S'14–M'16) received the B.S. degree in mechanical and electronics engineering from the Beijing Institute of Technology, Beijing, China, in 2005, the M.S. degree in software engineering from Peking University, Beijing, China, in 2009, and the Ph.D. degree in computer engineering from the Electromagnetic Compatibility Laboratory, Missouri University of Science and Technology, Rolla, MO, USA, in 2015.

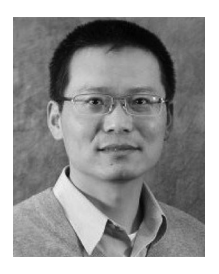
Starting from 2015, he was with Cisco Systems and Hewlett-Packard as a Hardware Engineer. Since

2018, he has been a Senior Hardware Engineer with Alibaba Infrastructure Service, Alibaba Group (U.S.) Inc., Sunnyvale, CA, USA. His research interests include high-speed signal integrity and power integrity in data center industries.



Bidyut Sen received the Ph.D. degree in physics from the State University of New York, Stony Brook, NY, USA

He is a Principal Engineer with the Unified Compute Server Group, Cisco Systems, Inc. He has many years of experience in the computer industry and has worked in several companies including Sun Microsystems, Fujitsu, and LSI Logic. He has several publications, presentations, and patents.



Jun Fan (S'97–M'00–SM'06–F'16) received the B.S. and M.S. degrees in electrical engineering from Tsinghua University, Beijing, China, in 1994 and 1997, respectively, and the Ph.D. degree in electrical engineering from the University of Missouri—Rolla (now Missouri University of Science and Technology), Rolla, MO, USA, in 2000.

From 2000 to 2007, he was with NCR Corporation, San Diego, CA, USA, as a Consultant Engineer. In July 2007, he joined the Missouri University of Science and Technology, where he is currently a

Professor and Director with the Missouri S&T, Electromagnetic Compatibility Laboratory. He is also the Director of the National Science Foundation Industry/University Cooperative Research Center for Electromagnetic Compatibility and a Senior Investigator with Missouri S&T Material Research Center. His research interests include signal integrity and EMI designs in high-speed digital systems, dc power-bus modeling, intrasystem EMI and RF interference, PCB noise reduction, differential signaling, and cable/connector designs.

Dr. Fan was the recipient of the IEEE EMC Society Technical Achievement Award in August 2009. He was the Chair of the IEEE EMC Society TC-9 Computational Electromagnetics Committee from 2006 to 2008, and was a Distinguished Lecturer of the IEEE EMC Society in 2007 and 2008, respectively. He is currently the Chair of the Technical Advisory Committee of the IEEE EMC Society, and is an Associate Editor for the IEEE TRANSACTIONS ON ELECTROMAGNETIC COMPATIBILITY and the EMC Magazine.